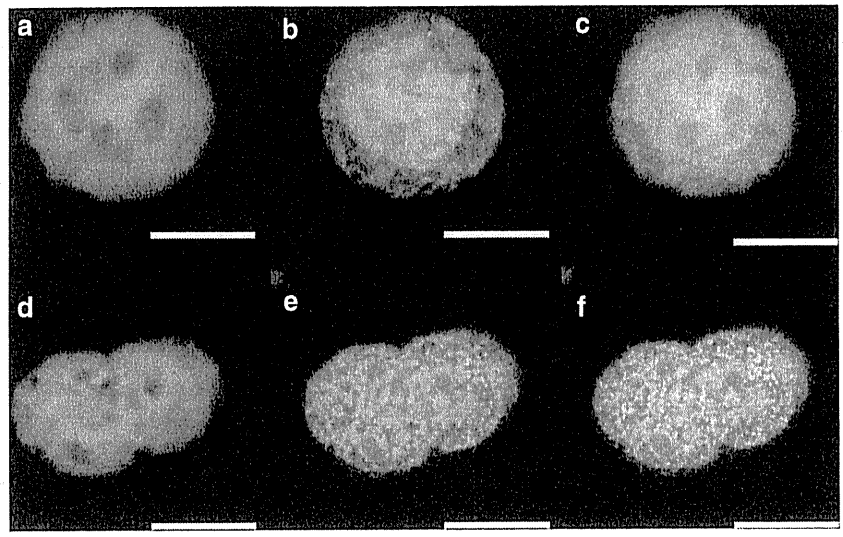

Figure 1 Distribution of FITC-labled NF-κB decoy oligodeoxynucleotide (ODN) by LM8 cells cultured in alginate beads. LM8 cells cultured in alginate beads were transfected with 'naked' fluorescein isothiocianate (FITC)-labeled NF-κB decoy ODN (green) for 4 h. Nuclei were stained with propidium iodide (red). The transfection efficiency was ~100%. FITC-fluorescence was also confirmed in the nuclei of dividing LM8 cells. (**a**, **d**): nuclear stain; (**b**, **e**): FITC-labeled decoy; (**c**, **f**): overlay. Scale bar: 10 μm. The color reproduction of this figure is available on the html full text version of the manuscript.

DNA-binding capacity of NF-κB was evaluated using a p65 enzyme-linked immunosorbent assay (ELISA).[26] The LM8 parent Dunn cell line[22] was also evaluated. The NF-κB (p65) signaling activity of untreated LM8 cells (control) was significantly higher ($P<0.01$), about threefold, than that of the Dunn cells (Figure 2). Treatment with NF-κB decoy ODN suppressed the NF-κB signaling activity of LM8 cells in a dose-dependent manner (percentage of control; SCD: $-14.0\pm4.9\%$, $P<0.05$; decoy (100 nM): $-27.7\pm10.3\%$, $P<0.01$; decoy (10 μM): $-74.5\pm3.1\%$, $P<0.01$). Importantly, compared with the parent Dunn cell line, the activation of NF-κB (p65) by the LM8 cell line was significantly ($P<0.05$) suppressed by transfection of 10 μM NF-κB decoy ODN (decoy (10 μM): $-74.5\pm3.1\%$; Dunn: $-61.7\pm2.8\%$; $P<0.05$; percentage of control).

Cell proliferation

The ELISA-based bromodeoxyuridine (BrdU) assay was used to evaluate the effect of NF-κB decoy ODN on the cell proliferation of LM8 osteosarcoma cells *in vitro*. The growth of LM8 osteosarcoma cells cultured in alginate beads was not affected by 2–7 days incubation with NF-κB decoy ODN or SCD (Figure 3). No significant differences were observed among the experimental groups throughout the experimental period.

mRNA expression of VEGF and ICAM-1

To examine the molecular mechanisms underlying the inhibitory action of NF-κB decoy ODN on metastasis by LM8 cells, VEGF and ICAM-1 mRNA was quantified by real-time PCR *in vitro*. At 24 h after inoculation of LM8 cells, the transfection of decoy (10 μM) induced a

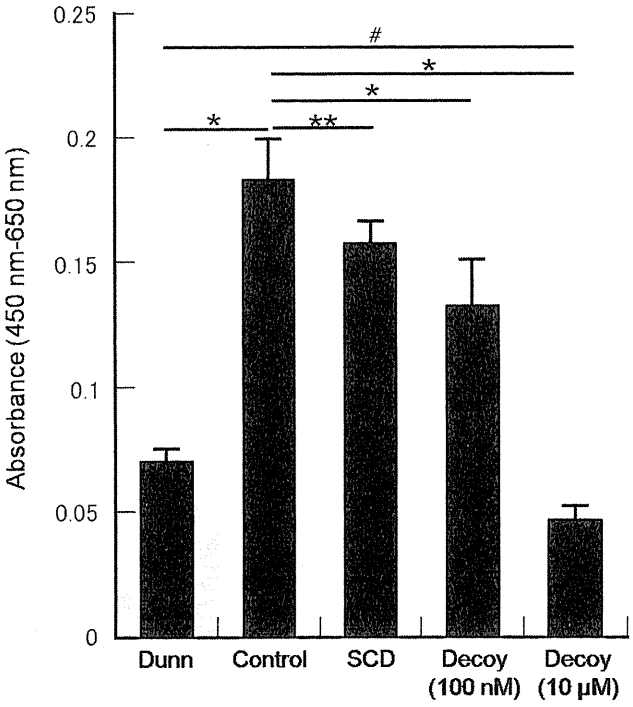

Figure 2 Effect of NF-κB decoy oligodeoxynucleotide (ODN) on the DNA binding capacity of NF-κB. The NF-κB DNA binding activity of each experimental group was evaluated using an NF-κB (p65) enzyme-linked immunosorbent assay (ELISA). (1) Dunn (Dunn cell line) (serum-free medium), (2) LM8 cells (serum-free medium), (3) Scrambled decoy ODN at 100 nM (SCD), (4) NF-κB decoy ODN at 100 nM (Decoy 100 nM) and (5) NF-κB decoy ODN at 10 μM (Decoy 10 μM). $^{**}P<0.05$ and $^{*}P<0.01$, compared with the untreated LM8 cells. $^{\#}P<0.01$, compared with the 10 μM group.

significant reduction of mRNA levels of *VEGF* genes compared with the other groups (Figure 4a) (percentage of control; SCD: $+12.7 \pm 2.1\%$; Decoy (100 nM): $+0.7 \pm 2.7\%$; Decoy (10 μM): $-31.2 \pm 3.1\%$, $P<0.01$). Similarly, the expression of the *ICAM-1* gene was markedly decreased in the 10 μM group compared with the other groups (Figure 4b) (percentage of control; SCD: $-0.3 \pm 9.1\%$; Decoy (100 nM): $-5.9 \pm 10.8\%$; Decoy (10 μM): $-34.3 \pm 2.6\%$, $P<0.01$).

Cell detachment assay

The parental Dunn cell line and its derivative LM8 encapsulated in an alginate bead culture system were able to grow in a three-dimensional structure with cells detaching from the alginate environment. The number of detached cells was greater in the LM8 cell line than in the Dunn cell line, suggesting that the cell kinetics in this culture system reflect the *in vivo* malignancy potential of the cells.[23] To evaluate the effect of the NF-κB decoy ODN on the metastatic potential *in vitro* using this culture system, the number of cells detaching from the alginate bead and adhering to the bottom of the culture plate was quantified. On day 1 of culture, detached cells were found only in the control group. The number of cells detaching from alginate beads increased with time in all experimental groups, however, the number of detached cells for the Decoy (10 μM) group was significantly ($P<0.05$) lower than that of the control group on day 7 (Figure 5a). Representative images on day 7 of culture show that clumps of LM8 cells were found in the control group (Figure 5b), whereas only solitary cells were identified in the decoy (10 μM) group (Figure 5c).

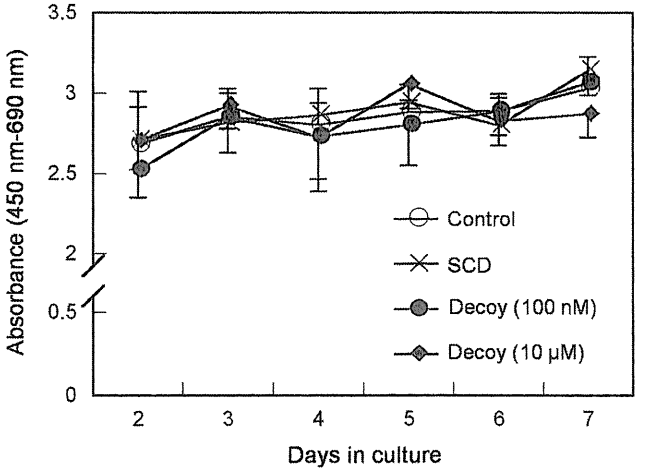

Figure 3 Effect of NF-κB decoy oligodeoxynucleotide on the cell proliferation of LM8 cells. The cell proliferation of LM8 cells cultured for 2–7days in alginate beads was analyzed by a bromodeoxyuridine (BrdU) assay. No significant differences were observed among the experimental groups.

In vivo *alginate transplantation study*

To examine the inhibitory effect of NF-κB decoy ODN on pulmonary metastasis *in vivo*, alginate beads containing LM8 cells pre-transfected with NF-κB decoy ODN were transplanted into the dorsal skin of mice. In a preliminary experiment,[23] beads containing murine OS cells, either the parental Dunn cell line or its derivative cell line LM8, were transplanted into the dorsal skin of mice to determine their metastatic potential *in vivo*. The rate of pulmonary metastasis was higher for LM8 cells than Dunn cells, suggesting that the metastatic potential of cells in alginate bead culture reflect the original *in vivo* potential.

In this study, tumor nodules were formed in all mice in both the control (10/10) and SCD (10/10) groups. However, subcutaneous tumor nodules were formed in 90% of mice by both the decoy 100 nM (9/10) and 10 μM (9/10) groups. Tumor nodules of all groups progressively increased in volume until the mice was killed on day 35 after transplantation. There were no significant

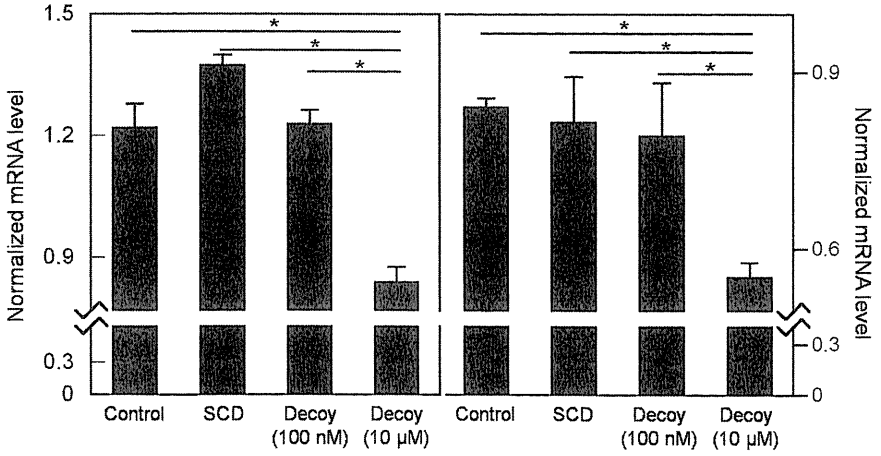

Figure 4 Effects of NF-κB decoy oligodeoxynucleotide on the mRNA expression of vascular endothelial growth factor (VEGF: **a**) and intercellular adhesion molecule-1 (ICAM-1: **b**). VEGF and ICAM-1 mRNA levels were quantified by real-time PCR and normalized by the glyceraldehyde-3-phosphate dehydrogenase (GAPDH) level of each sample. *$P<0.01$, compared with the Decoy (10 μM) group. SCD, scrambled decoy ODN (100 nM).

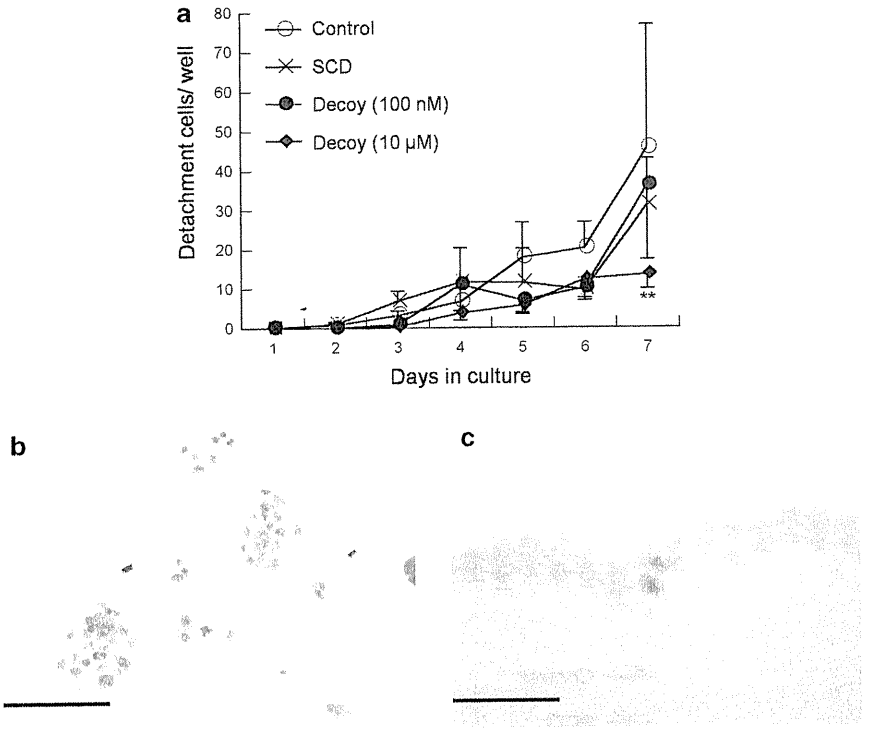

Figure 5 Effects of NF-κB decoy oligodeoxynucleotide on cell detachment from alginate beads. LM8 cells that detached from alginate beads during 24 h were stained with Hematoxylin and manually counted under a light microscope (**a**). Representative light microscopy images of Control (**b**) and Decoy 10 μM groups (**c**) on day 7 are shown. Scale bars: 200 μm. $^{**}P<0.05$, compared with Control group.

differences in tumor volume (Figure 6a) and body weight (Figure 6b) among all groups throughout the experimental period. Representative histological images of the lungs removed from each experimental group are shown in Figure 7. Microscopic analysis of the lungs found metastatic lesions in all the experimental groups. A large number of tumor nodules were found in the lungs of the control and SCD groups. Tumor nodules of the control and SCD groups were larger than those of the NF-κB decoy ODN at 100 nM and 10 μM groups. There was a marked reduction in the number of metastatic tumors produced by LM8 cells transfected with NF-κB decoy ODN at 10 μM (Figure 8) (percentage of control; SCD: 138.2 ± 35.7, Decoy 100 nM: 81.7 ± 19.6, Decoy 10 μM: 37.3 ± 15.8, $P<0.05$ vs control, $P<0.01$ vs SCD).

Discussion

The results of our study show that NF-κB was constitutively activated in a murine osteosarcoma cell line LM8, which has a higher pulmonary metastatic potential than its parental Dunn cell line. Furthermore, the level of NF-κB activation was significantly higher in the LM8 cell line than the Dunn cell line. This increased activation of NF-κB is considered to contribute to the maintenance of a highly proliferative malignant phenotype. In this study, naked NF-κB decoy ODN was successfully transfected into the nuclei of LM8 cells cultured using three-dimensional alginate beads, and suppressed the NF-κB signaling pathway. Transfection of NF-κB decoy ODN at 10 μM decreased the detachment of cells from the alginate beads and suppressed the expression of such metastasis-related genes as VEGF and ICAM-1. In the *in vivo* alginate transplantation study, the number of pulmonary metastases was markedly decreased by transfection of NF-κB decoy ODN.

In a preliminary study, we used two concentrations of scrambled decoy ODN (SCD; 100 nM and 10 μM) to exclude the possibility of any non-specific effects of ODN on cell proliferation and mRNA expression assays *in vitro*. In both assays, significant differences were not found between the control group and the SCD groups (at either 100 nM or 10 μM). Therefore, for this study, we selected the 100 nM concentration of SCD for use as the ODN control (SCD group).

The transfection efficiency study confirmed that 'naked' NF-κB decoy ODN was transfected into the nuclei of LM8 cells cultured in an alginate bead three-dimensional culture system. Suzuki *et al.*[29] reported that NF-κB decoy ODN was successfully and efficiently transfected into human osteosarcoma cells after enzymatic removal of the extracellular matrix in monolayer culture. In this study, we have successfully transfected 'naked' NF-κB decoy ODN into LM8 cells in a three-dimensional alginate environment. We speculated that NF-κB decoy ODN could be transfected into LM8 cells suspended in alginate environment before formation of an extracellular matrix and/or cell-to-cell adhesion, proving

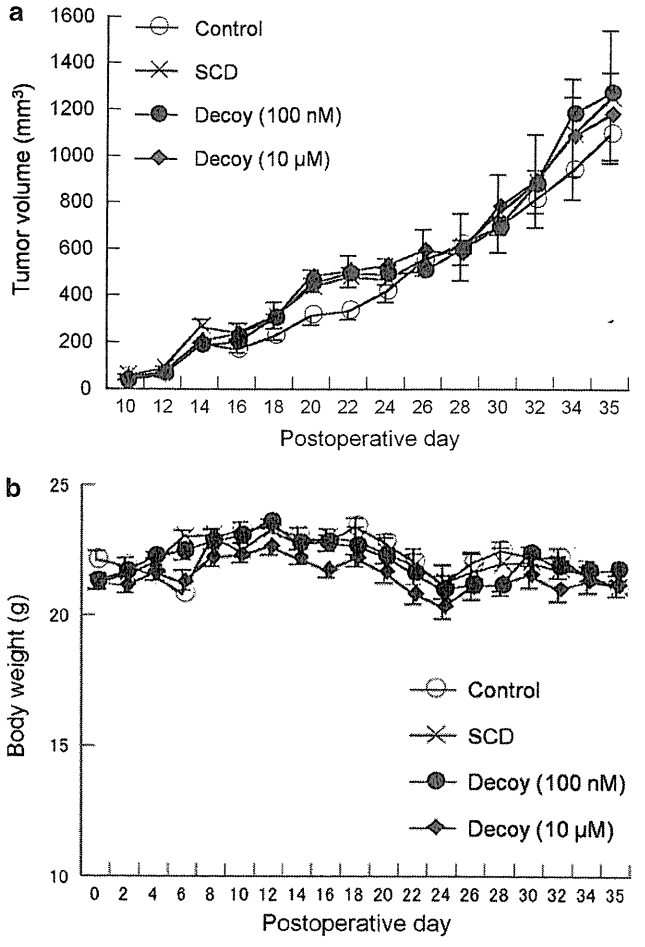

Figure 6 Effects of NF-κB decoy oligodeoxynucleotide on local tumor volume (**a**) and weight of mice (**b**) *in vivo*. Five alginate beads ($\sim 2.0 \times 10^5$ LM8 cells) were transplanted subcutaneously into the dorsal skin of 10 mice in each experimental group. Tumor volume and weight were measured every other day. There were no significant differences in tumor volume or body weight.

the advantage of using a three-dimensional culture system. The results of this study showed that activation of NF-κB signaling activity was markedly suppressed by transfection of NF-κB decoy ODN in a dose-dependent manner; suggesting that NF-κB signaling activity can be effectively suppressed by transfection of NF-κB decoy ODN.

It has been reported that activation of NF-κB causes certain types of malignant tumor cells to suppress apoptosis.[30,31] Therefore, apoptosis should be induced when NF-κB signaling is inhibited.[32] In human osteosarcoma, genes relating to apoptosis exist in the downstream of NF-κB signaling.[33] Asai *et al.*[14] showed in an *in vitro* study that transfecting valosin-containing protein (VCP; an inactivator of inhibitor-κB) into osteosarcoma cells significantly decreased the rate of apoptosis compared with non-treated osteosarcoma cells. In our study, the DNA-binding activity of NF-κB by LM8 cells was markedly inhibited by transfection of NF-κB decoy ODN. However, the BrdU assay showed that NF-κB decoy ODN did not affect the cell proliferative activity of LM8. This finding suggests that the NF-κB signaling pathway may not have been completely blocked by the transfection of NF-κB decoy ODN. Alternatively, other anti-apoptosis signals, such as Bcl-2, murine double minute 2 (MDM2), DNA-dependent protein kinase (DNA-PK) and epidermal growth factor receptor (EGFR) might be involved.[34]

The capacity for angiogenesis and adhesion in distant organs is a crucial factor enabling distant metastasis of malignant tumors.[35] VEGF has been reported to induce the proliferation of endothelial cells and increased vascular permeability,[10] whereas ICAM-1 is known to have an important role in lymphatic and vascular invasion, and subsequent adhesion to other tissues.[36] It has been reported that the expression of VEGF and/or ICAM-1 is correlated to the malignancy, or metastatic potential of tumors including osteosarcoma.[37,38] In our study, the mRNA levels of VEGF and ICAM-1 were significantly decreased by transfection of NF-κB decoy ODN, indicating that the metastatic potential of LM8 cells was decreased by the transfection of NF-κB decoy ODN.

We evaluated the number of cells detached from alginate beads because the detachment observed in this culture system may reflect the initial step of metastasis.[23,39] The number of detached cells was significantly reduced by transfection of NF-κB decoy ODN at 10 μM. This result leads us to speculate that the cellular kinetics related to migration or invasion was inhibited by administration of NF-κB decoy ODN. Next, the *in vivo* study demonstrated that although tumor volume was not reduced, the number of pulmonary metastases was significantly reduced by transfection with NF-κB decoy ODN at 10 μM. As with the *in vitro* results, transfection with NF-κB decoy ODN did not affect the activity of cell proliferation, but did alleviate the metastatic potential of LM8 cells *in vivo*. Similarly, Kawamura *et al.*[21] reported that combined treatment of NF-κB decoy ODN with an anti-cancer drug did not suppress tumor cell proliferation, but did reduce hepatic metastasis in a mouse tumor model. Taken together, these results suggest that cytokines regulated by NF-κB may have pivotal roles in the process of metastasis.

The clinical application of NF-κB decoy ODN is hampered by the instability of oligonucleotides in blood and their rapid degradation by nuclease.[40,41] The intravenous injection of 'naked' NF-κB decoy ODN in an animal model showed accumulation in the kidney (30% of the dose per g tissue), but little accumulation in other organs.[42] Therefore, alternative delivery methods such as local administration,[43,44] combination use with cationic liposome as a carrier,[40] and physical stimulation by ultrasound wave[45,46] have been reported. In other series of study, we directly injected 'naked' NF-κB decoy ODN into a LM8 tumor mass and examined the biodistribution and the inhibitory effects of the decoy in a murine spontaneous pulmonary metastasis model.[47] The results demonstrated that NF-κB decoy ODN was transfected only into cells marginal to the tumor and no inhibitory

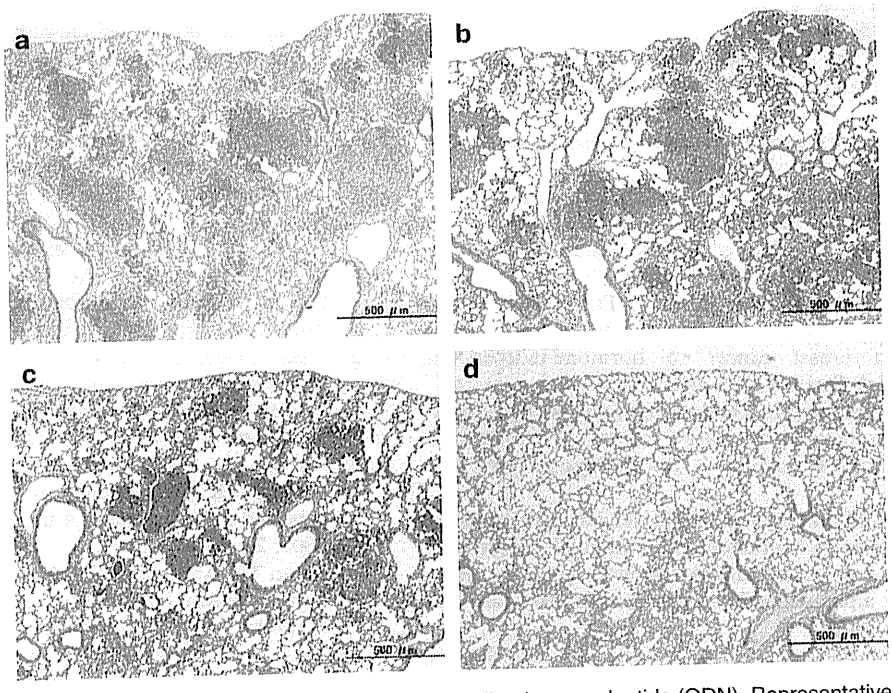

Figure 7 Histological images of lungs after transfection of NF-κB decoy oligodeoxynucleotide (ODN). Representative light microscopy images of lungs removed from each experimental group are shown, where (**a**) Control, (**b**) SCD, (**c**) NF-κB decoy ODN 100 nM and (**d**) NF-κB decoy ODN 10 μM. Larger numbers of tumor nodules were found in the lungs of the control and SCD groups, the number of nodules was markedly reduced in the decoy-transfected groups. SCD, scrambled decoy ODN (100 nM). Scale bar: 500 μm.

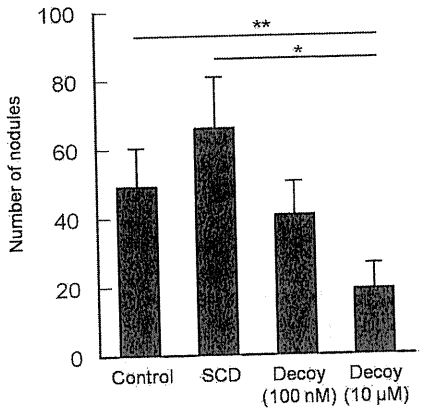

Figure 8 Effect of NF-κB decoy oligodeoxynucleotide on pulmonary metastasis of LM8 osteosarcoma in *in vivo*. The number of tumor nodules (pulmonary metastases) in the maximal area of each lung section was counted microscopically. $^{*}P<0.01$ compared with SCD group, $^{**}P<0.05$, compared with control group. SCD, scrambled decoy ODN (100 nM).

effects on pulmonary metastasis were observed. For clinical applications, effective transfection methods to place decoy ODN into tumor cells are needed.

In conclusion, we successfully transfected 'naked' NF-κB decoy ODN into LM8 cells cultured in an alginate-encapsulated tumor spheroid model. The DNA-binding capacity of NF-κB by LM8 cells was significantly suppressed by transfection of NF-κB decoy ODN. In the *in vivo* alginate bead transplant study, pulmonary metastases were significantly reduced by transfection of NF-κB decoy ODN. The results on cell proliferation and mRNA expression of VEGF and ICAM-1 *in vitro* provide biological evidence for the mechanism for inhibition of pulmonary metastasis by LM8 cells. Our results suggest that NF-κB has crucial and specific roles in the regulation of tumor metastasis and may be an important therapeutic target for the development of anti-metastatic treatment for osteosarcoma.

Conflict of interest

The authors declare no conflict of interest.

Acknowledgements

We thank Takahiro Iino and Kei Chiba for their technical assistance. This study was sponsored by grants from the Uehara Memorial Life Science Foundation and from the Ministry of Education, Culture, Sports, Science and Technology (Japan).

References

1 Uchida A, Myoui A, Araki N, Yoshikawa H, Shinto Y Ueda T. Neoadjuvant chemotherapy for pediatric osteosarcoma patients. *Cancer* 1997; **79**: 411–415.

2 Thanos D, Maniatis T. NF-kappa B: a lesson in family values. *Cell* 1995; **80**: 529–532.
3 Baldwin Jr AS. The NF-kappa B and I kappa B proteins: new discoveries and insights. *Annu Rev Immunol* 1996; **14**: 649–683.
4 Ravi R, Bedi A. NF-kappaB in cancer—a friend turned foe. *Drug Resist Updat* 2004; **7**: 53–67.
5 Meyskens Jr FL, Buckmeier JA, McNulty SE, Tohidian NB. Activation of nuclear factor-kappa B in human metastatic melanoma cells and the effect of oxidative stress. *Clin Cancer Res* 1999; **5**: 1197–1202.
6 Nakshatri H, Bhat-Nakshatri P, Martin DA, Goulet Jr RJ, Sledge Jr GW. Constitutive activation of NF-kappaB during progression of breast cancer to hormone-independent growth. *Mol Cell Biol* 1997; **17**: 3629–3639.
7 Yokoo T, Kitamura M. Dual regulation of IL-1 beta-mediated matrix metalloproteinase-9 expression in mesangial cells by NF-kappa B and AP-1. *Am J Physiol* 1996; **270**: F123–F130.
8 Yoshida S, Ono M, Shono T, Izumi H, Ishibashi T, Suzuki H *et al.* Involvement of interleukin-8, vascular endothelial growth factor, and basic fibroblast growth factor in tumor necrosis factor alpha-dependent angiogenesis. *Mol Cell Biol* 1997; **17**: 4015–4023.
9 Park BK, Zhang H, Zeng Q, Dai J, Keller ET, Giordano T *et al.* NF-kappaB in breast cancer cells promotes osteolytic bone metastasis by inducing osteoclastogenesis via GM-CSF. *Nat Med* 2007; **13**: 62–69.
10 Huang S, Pettaway CA, Uehara H, Bucana CD, Fidler IJ. Blockade of NF-kappaB activity in human prostate cancer cells is associated with suppression of angiogenesis, invasion, and metastasis. *Oncogene* 2001; **20**: 4188–4197.
11 Huang S, DeGuzman A, Bucana CD, Fidler IJ. Nuclear factor-kappaB activity correlates with growth, angiogenesis, and metastasis of human melanoma cells in nude mice. *Clin Cancer Res* 2000; **6**: 2573–2581.
12 Andela VB, Sheu TJ, Puzas EJ, Schwarz EM, O'Keefe RJ, Rosier RN. Malignant reversion of a human osteosarcoma cell line, Saos-2, by inhibition of NFkappaB. *Biochem Biophys Res Commun* 2002; **297**: 237–241.
13 Andela VB, Siddiqui F, Groman A, Rosier RN. An immunohistochemical analysis to evaluate an inverse correlation between Runx2/Cbfa1 and NF kappa B in human osteosarcoma. *J Clin Pathol* 2005; **58**: 328–330.
14 Asai T, Tomita Y, Nakatsuka S, Hoshida Y, Myoui A, Yoshikawa H *et al.* VCP (p97) regulates NFkappaB signaling pathway, which is important for metastasis of osteosarcoma cell line. *Jpn J Cancer Res* 2002; **93**: 296–304.
15 Harimaya K, Tanaka K, Matsumoto Y, Sato H, Matsuda S, Iwamoto Y. Antioxidants inhibit TNFalpha-induced motility and invasion of human osteosarcoma cells: possible involvement of NFkappaB activation. *Clin Exp Metastasis* 2000; **18**: 121–129.
16 Kishida Y, Yoshikawa H, Myoui A. Parthenolide, a natural inhibitor of Nuclear Factor-kappaB, inhibits lung colonization of murine osteosarcoma cells. *Clin Cancer Res* 2007; **13**: 59–67.
17 Mori K, Le Goff B, Berreur M, Riet A, Moreau A, Blanchard F *et al.* Human osteosarcoma cells express functional receptor activator of nuclear factor-kappa B. *J Pathol* 2007; **211**: 555–562.
18 Morishita R, Sugimoto T, Aoki M, Kida I, Tomita N, Moriguchi A *et al. In vivo* transfection of cis element 'decoy' against nuclear factor-kappaB binding site prevents myocardial infarction. *Nat Med* 1997; **3**: 894–899.
19 Morishita R, Tomita N, Kaneda Y, Ogihara T. Molecular therapy to inhibit NFkappaB activation by transcription factor decoy oligonucleotides. *Curr Opin Pharmacol* 2004; **4**: 139–146.
20 Kawamura I, Morishita R, Tomita N, Lacey E, Aketa M, Tsujimoto S *et al.* Intratumoral injection of oligonucleotides to the NF kappa B binding site inhibits cachexia in a mouse tumor model. *Gene Ther* 1999; **6**: 91–97.
21 Kawamura I, Morishita R, Tsujimoto S, Manda T, Tomoi M, Tomita N *et al.* Intravenous injection of oligodeoxynucleotides to the NF-kappaB binding site inhibits hepatic metastasis of M5076 reticulosarcoma in mice. *Gene Ther* 2001; **8**: 905–912.
22 Asai T, Ueda T, Itoh K, Yoshioka K, Aoki Y, Mori S *et al.* Establishment and characterization of a murine osteosarcoma cell line (LM8) with high metastatic potential to the lung. *Int J Cancer* 1998; **76**: 418–422.
23 Akeda K, Nishimura A, Satonaka H, Shintani K, Kusuzaki K, Matsumine A *et al.* Three-dimensional alginate spheroid culture system of murine osteosarcoma. *Oncol Rep* 2009; **22**: 997–1003.
24 Dunn TB, Andervont HB. Histology of some neoplasms and non-neoplastic lesions found in wild mice maintained under laboratory conditions. *J Natl Cancer Inst* 1963; **31**: 873–901.
25 Masuda K, Takegami K, An H, Kumano F, Chiba K, Andersson GB *et al.* Recombinant osteogenic protein-1 upregulates extracellular matrix metabolism by rabbit annulus fibrosus and nucleus pulposus cells cultured in alginate beads. *J Orthop Res* 2003; **21**: 922–930.
26 Renard P, Ernest I, Houbion A, Art M, Le Calvez H, Raes M *et al.* Development of a sensitive multi-well colorimetric assay for active NFkappaB. *Nucleic Acids Res* 2001; **29**: E21.
27 Imai Y, Miyamoto K, An HS, Thonar EJ, Andersson GB, Masuda K. Recombinant human osteogenic protein-1 upregulates proteoglycan metabolism of human anulus fibrosus and nucleus pulposus cells. *Spine* 2007; **32**: 1303–1309;discussion 1310.
28 Matsumine A, Shintani K, Kusuzaki K, Matsubara T, Satonaka H, Wakabayashi T *et al.* Expression of decorin, a small leucine-rich proteoglycan, as a prognostic factor in soft tissue tumors. *J Surg Oncol* 2007; **96**: 411–418.
29 Horiuchi K, Morioka H, Nishimoto K, Suzuki Y, Susa M, Nakayama R *et al.* Growth suppression and apoptosis induction in synovial sarcoma cell lines by a novel NF-kappaB inhibitor, dehydroxymethylepoxyquinomicin (DHMEQ). *Cancer Lett* 2008; **272**: 336–344.
30 Wu JM, Sheng H, Saxena R, Skill NJ, Bhat-Nakshatri P, Yu M *et al.* NF-kappaB inhibition in human hepatocellular carcinoma and its potential as adjunct to sorafenib based therapy. *Cancer Lett* 2009; **278**: 145–155.
31 Nishimura D, Ishikawa H, Matsumoto K, Shibata H, Motoyoshi Y, Fukuta M *et al.* DHMEQ, a novel NF-kappaB inhibitor, induces apoptosis and cell-cycle arrest in human hepatoma cells. *Int J Oncol* 2006; **29**: 713–719.
32 Horiguchi Y, Kuroda K, Nakashima J, Murai M, Umezawa K. Antitumor effect of a novel nuclear factor-kappa B activation inhibitor in bladder cancer cells. *Expert Rev Anticancer Ther* 2003; **3**: 793–798.
33 Zucchini C, Rocchi A, Manara MC, De Sanctis P, Capanni C, Bianchini M *et al.* Apoptotic genes as potential markers of metastatic phenotype in human osteosarcoma cell lines. *Int J Oncol* 2008; **32**: 17–31.
34 Um JH, Kwon JK, Kang CD, Kim MJ, Ju DS, Bae JH *et al.* Relationship between antiapoptotic molecules and metastatic potency and the involvement of DNA-dependent

protein kinase in the chemosensitization of metastatic human cancer cells by epidermal growth factor receptor blockade. *J Pharmacol Exp Ther* 2004; **311**: 1062–1070.

35 Folkman J. The role of angiogenesis in tumor growth. *Semin Cancer Biol* 1992; **3**: 65–71.

36 Huang WC, Chan ST, Yang TL, Tzeng CC, Chen CC. Inhibition of ICAM-1 gene expression, monocyte adhesion and cancer cell invasion by targeting IKK complex: molecular and functional study of novel alpha-methylene-gamma-butyrolactone derivatives. *Carcinogenesis* 2004; **25**: 1925–1934.

37 Lee YH, Tokunaga T, Oshika Y, Suto R, Yanagisawa K, Tomisawa M *et al.* Cell-retained isoforms of vascular endothelial growth factor (VEGF) are correlated with poor prognosis in osteosarcoma. *Eur J Cancer* 1999; **35**: 1089–1093.

38 Lin YC, Shun CT, Wu MS, Chen CC. A novel anticancer effect of thalidomide: inhibition of intercellular adhesion molecule-1-mediated cell invasion and metastasis through suppression of nuclear factor-kappaB. *Clin Cancer Res* 2006; **12**: 7165–7173.

39 Tannock IF, Hill RP, Bristow RG, Harrington L. Tumor Progressin and Metastasis: Cellular, Molecular, and Micro-environment Factors. In: Khokha R, Voura E, Hill RP (eds). *The Basic Science of Oncology*, Fourth edn The McGraw-Hill Companies, Inc.: New York, 2004, pp 205–230.

40 Roque F, Mon G, Belardi J, Rodriguez A, Grinfeld L, Long R *et al.* Safety of intracoronary administration of c-myc antisense oligomers after percutaneous transluminal coronary angioplasty (PTCA). *Antisense Nucleic Acid Drug Dev* 2001; **11**: 99–106.

41 Miyao T, Takakura Y, Akiyama T, Yoneda F, Sezaki H, Hashida M. Stability and pharmacokinetic characteristics of oligonucleotides modified at terminal linkages in mice. *Antisense Res Dev* 1995; **5**: 115–121.

42 Higuchi Y, Kawakami S, Oka M, Yabe Y, Yamashita F, Hashida M. Intravenous administration of mannosylated cationic liposome/NFkappaB decoy complexes effectively prevent LPS-induced cytokine production in a murine liver failure model. *FEBS Lett* 2006; **580**: 3706–3714.

43 De Vry CG, Prasad S, Komuves L, Lorenzana C, Parham C, Le T *et al.* Non-viral delivery of nuclear factor-kappaB decoy ameliorates murine inflammatory bowel disease and restores tissue homeostasis. *Gut* 2007; **56**: 524–533.

44 Desmet C, Gosset P, Pajak B, Cataldo D, Bentires-Alj M, Lekeux P *et al.* Selective blockade of NF-kappa B activity in airway immune cells inhibits the effector phase of experimental asthma. *J Immunol* 2004; **173**: 5766–5775.

45 Inagaki H, Suzuki J, Ogawa M, Taniyama Y, Morishita R, Isobe M. Ultrasound-microbubble-mediated NF-kappaB decoy transfection attenuates neointimal formation after arterial injury in mice. *J Vasc Res* 2006; **43**: 12–18.

46 Azuma H, Tomita N, Sakamoto T, Kiyama S, Inamoto T, Takahara K *et al.* Marked regression of liver metastasis by combined therapy of ultrasound-mediated NF kappaB-decoy transfer and transportal injection of paclitaxel, in mouse. *Int J Cancer* 2008; **122**: 1645–1656.

47 Matsubara T, Akeda K, Nishimura A, Kusuzaki K, Matsumine A, Shintani K *et al.* Injection of naked decoy oligodeoxynucleotide against nuclear factor-kappa B into a murine osteosarcoma in a spontaneous pulmonary metastasis model. *Trans Orthop Res Soc* 2008; **33**: 1196.

Int J Clin Oncol (2011) 16:101–108
DOI 10.1007/s10147-011-0217-3

REVIEW ARTICLE

A novel hyperthermia treatment for bone metastases using magnetic materials

Akihiko Matsumine · Kenji Takegami · Kunihiro Asanuma · Takao Matsubara · Tomoki Nakamura · Atsumasa Uchida · Akihiro Sudo

Received: 9 February 2011 / Published online: 4 March 2011

Abstract Patients with bone metastases in the extremities sometimes require surgical intervention to prevent deterioration of quality of life due to a pathological fracture. The use of localized radiotherapy combined with surgical reinforcement has been a gold standard for the treatment of bone metastases. However, radiotherapy sometimes induces soft tissue damage, including muscle induration and joint contracture. Moreover, cancer cells are not always radiosensitive. Hyperthermia has been studied since the 1940s using an experimental animal model to treat various types of advanced cancer, and studies have now reached the stage of clinical application, especially in conjunction with radiotherapy or chemotherapy. Nevertheless, bone metastases have several special properties which discourage oncologists from developing hyperthermic therapeutic strategies. First, the bone is located deep in the body, and has low thermal conductivity due to the thickness of cortical bone and the highly vascularized medulla. To address these issues, we developed new hyperthermic strategies which generate heat using magnetic materials under an alternating electromagnetic field, and started clinical application of this treatment modality. The purpose of this review is to summarize the latest studies on hyperthermic treatment in the field of musculoskeletal tumors, and to introduce the treatment strategy employing our novel hyperthermia approach.

Keywords Hyperthermia · Bone metastasis · Pathological fracture · Magnetic material · Electromagnetic field

A. Matsumine (✉) · K. Asanuma · T. Matsubara · T. Nakamura · A. Uchida · A. Sudo
Department of Orthopaedic Surgery,
Mie University Graduate School of Medicine,
2-174, Edobashi, Tsu, Mie 514-8507, Japan
e-mail: matsumin@clin.medic.mie-u.ac.jp

K. Takegami
Department of Orthopaedic Surgery,
Saiseikai Matsusaka General Hospital,
15-6 Asahi-chyo 1-ku, Matsusaka,
Mie 515-8557, Japan

Introduction

Bone is the most common site of cancer metastasis, and is particularly important in breast and prostate cancers because these diseases have a high prevalence of bone metastases. At postmortem examination, ~70% of patients dying of these cancers have evidence of metastatic bone disease. Cancers of the thyroid, kidneys, and lungs also commonly give rise to bone metastases with an incidence of 30–40% at postmortem examination [1].

Patients with bone metastases in the extremities sometimes require surgical intervention to prevent deterioration of quality of life due to pathological fractures, which commonly occur as a result of lytic lesions in weight-bearing bones. Destruction of both cortical and trabecular bone is structurally important. Fractures are highly unlikely to occur (2.3%) when less than 50% of the cortex is destroyed, and are most likely to occur (80%) when over 75% of the cortex is destroyed [2].

Radiotherapy is generally a safe and effective treatment modality, and is well established for patients with bone metastases. However, radiotherapy without surgical reinforcement cannot prevent pathological fractures in patients presenting with impending fractures of long tubular bones. The addition of internal fixation before localized radiotherapy can reduce the risk of further bone destruction,

which leads to increased pain, loss of fixation, and the need for additional orthopedic procedures [3, 4]. Radiotherapy also sometimes induces soft tissue damage, including muscle induration and joint contracture [4]. Moreover, cancer cells are not always radiosensitive. Better methods are therefore needed to treat patients with bone metastases. We have developed a novel hyperthermic strategy which generates heat using magnetic materials under an alternating electromagnetic field to treat bone metastases, and have started clinical applications of this treatment modality.

The purpose of this review is to summarize the use of hyperthermic treatment in the field of musculoskeletal tumors, and to introduce our new treatment strategy using hyperthermia.

The history of therapeutic hyperthermia and the mechanisms of cancer cell death

Although there have been many references to the use of heat to treat human cancer, dating back to the writings of Hippocrates, the scientific approach to hyperthermia has been studied since the 1940s [5]. Hyperthermia can be applied by several methods: local hyperthermia by external or internal energy sources, regional hyperthermia by perfusion of organs or limbs, or by irrigation of body cavities, and whole body hyperthermia [5].

There is a clear rationale for using hyperthermia in cancer treatment. Recent progress in cell biology has revealed that hyperthermia, variously reported between 40 and 45°C, triggers tumor cell death by apoptosis, although the exact temperature differs depending on the individual conditions [6, 7]. Treatment at temperatures between 40 and 45°C is cytotoxic for cells in an environment with a low pO_2 and low pH conditions, which are usually found within tumor tissue due to the insufficient blood supply [5]. It is now well-known that hyperthermia-induced apoptosis is characterized by the occurrence of intra-nucleosomal DNA cleavage [8]. Furthermore, recent experiments revealed that hyperthermia can increase tumor immunogenicity by stimulating antigen-presenting cells through heat shock proteins secreted from lysed tumor cells [5].

The clinical value of hyperthermia, in addition to other treatment modalities, has been shown in randomized trials. For example, significant improvements in clinical outcome have been demonstrated for tumors of the head and neck, breast, brain, bladder, cervix, rectum, lung, esophagus, prostate, vulva and vagina, and also for melanoma, especially in conjunction with radiotherapy or chemotherapy [5, 9, 10]. In the field of bone metastases, Fan et al. [11] reported that 57 of 62 patients treated with intra-operative microwave-induced hyperthermic treatment had shown excellent local control. Sakurai et al. [12] reported that hyperthermic treatment combined with external radiation therapy improved local control in thirteen patients with primary non-small cell lung cancer directly invading to bone.

However, the bone has several special properties which discourage oncologists from developing hyperthermic therapeutic strategies for bone metastasis. Heating of the tumor is usually achieved by means of external sources such as microwaves, ultrasound or a water bath [5]. However, even if these external sources are applied for bone metastases, it is difficult to achieve enough heat conduction to the tumor because the bone is located deep in the body and has low thermal conductivity, with a highly vascularized medulla. However, hyperthermia for bone tumors can be achieved using the polymerization heat of polymethylmethacrylate bone cement as a hyperthermic treatment [13, 14]; however, the generated heat tends to be unreliable and insufficient to reduce bone tumor growth [15]. Microwave-induced hyperthermia [11], laser-induced thermotherapy [16], and radiofrequency ablation [17] have been recently used, especially for spinal and pelvic metastasis. However, these therapeutic modalities are unsatisfactory for lesions located in the long tubular bones of the limbs, because pathological fractures cannot be prevented without surgical reinforcement of the bone lesion.

We therefore developed a new hyperthermic therapeutic strategy that uses magnetic materials for metastatic bone tumors based on experimental studies [15, 18–20], and have also started clinical investigations [21].

Novel hyperthermia induced using magnetic materials

The unique feature of magnetic materials is their reaction to a magnetic field. Physical energy conversion occurs in an alternating magnetic field, and hysteresis loss is a very important feature of magnetic materials, because it enables effective hyperthermia.

The concept of hyperthermic cancer therapy that utilizes magnetic materials and an alternating magnetic field has been proposed by many researchers [22–24]. Yan et al. showed that treatment using Fe_2O_3 nanoparticles combined with magnetic field hyperthermia could inhibit not only the proliferation of cultured liver cancer cells, but also induce apoptosis of cultured liver cancer cells. Moreover, they showed that this hyperthermic strategy has a significant inhibitory effect on the weight and volume of xenograft liver cancer [25]. Similarly, Hilger et al. [26] showed the feasibility of thermal ablation of breast cancer with magnetic nanoparticles using an animal model. Johannsen et al. [27] published the first report of the clinical application of hyperthermia for human cancer using magnetic

nanoparticles. They injected magnetic nanoparticle suspensions into the prostate under ultrasound and fluoroscopy guidance, and showed that hyperthermia using magnetic nanoparticles was feasible and well tolerated for a patient with previously irradiated and locally recurrent prostate carcinoma.

Localized hyperthermic treatment for musculoskeletal tumors with ferromagnetic ceramics was first reported by Kokubo [28] using an animal model. He made a bioactive and ferromagnetic glass ceramic by heat treatment of a Fe_2O_3–$CaO.SiO_2$–B_2O_3–P_2O_5 glass, and showed that this glass ceramic was useful as a thermoseed for hyperthermic treatment of cancer [28–31].

We modified these new hyperthermic strategies for use in treating bone metastases. First, we developed an alternating electromagnetic field generator (Yamamoto Vinita Co., Ltd., Osaka, Japan) [15, 18, 20]. The output power of the electromagnetic field was 7 kW, at a fixed frequency of 1.5 MHz. Exposure of the affected limb to the electromagnetic field can be achieved by inserting the limbs into a cylindrical coil of the generator (Fig. 1).

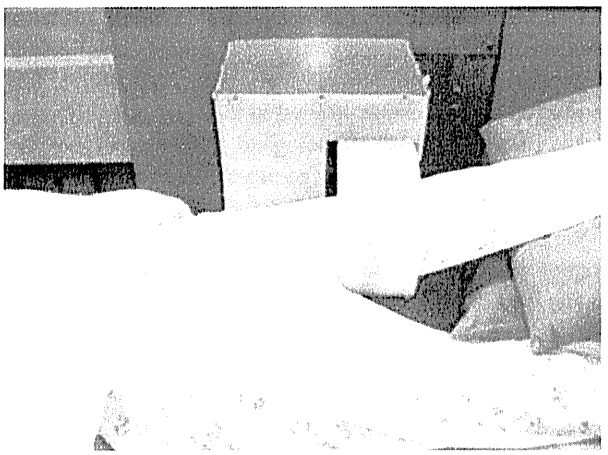

Fig. 1 Hyperthermia was postoperatively applied by inserting the affected limb into a cylindrical coil of the electromagnetic field generator

Next, we created a new bone cement made of glass ceramic that was partly replaced by magnetite (Fe_3O_4) powder [15, 18, 19], and examined the heat induction generated by hysteresis loss [18]. The composition of this material resembles the bioactive bone cement described by Kawanabe et al. [32], with a portion of the bioactive glass ceramic component replaced by magnetite. The temperature of this thermoseed rose in proportion to the weight ratio of magnetite powder, the volume of the thermoseed, and the intensity of the magnetic field. Furthermore, the heat induction in this thermoseed implanted into rabbit and human cadaver tibias was investigated by applying a magnetic field with a maximum of 300 Oe and 100 kHz. This system could easily produce heat in the thermoseed in bone beyond 50°C. When the temperature of the thermoseed in rabbit tibias was maintained at 50–60°C, the temperature at the bone surface rose to 43–45°C; but at a 10-mm distance from the thermoseed in the medullary canal, the temperature did not exceed 40°C (Fig. 2). These results demonstrate that ferromagnetic bone cement may be applicable for the hyperthermic treatment of bone tumors.

We next examined the antineoplastic effects of this treatment using an animal model. VX-2 tumors were transplanted into the tibia of rabbits. One week later, bone cement containing magnetite at a 60% weight ratio was implanted into the same site, followed by exposure to an alternating magnetic field for 50 min. We observed that the temperature of the tibia could rise to over 43°C, and that tumor growth was inhibited without any systemic adverse effects [20] (Fig. 3).

Since our first magnetite cement has not yet been approved by the Ministry of Health, Labour and Welfare of Japan, we decided to use a calcium phosphate cement

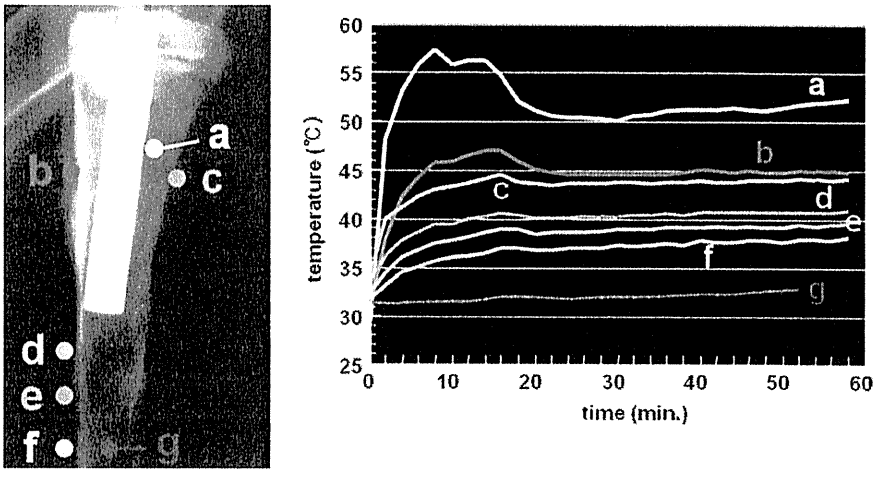

Fig. 2 Monitoring of the temperature at the various portions of a rabbit tibia. These data show the following: heat is easily generated on the surface of the magnetic material, the cortical bone has good heat conductivity, and the cancerous bone has poor heat conductivity

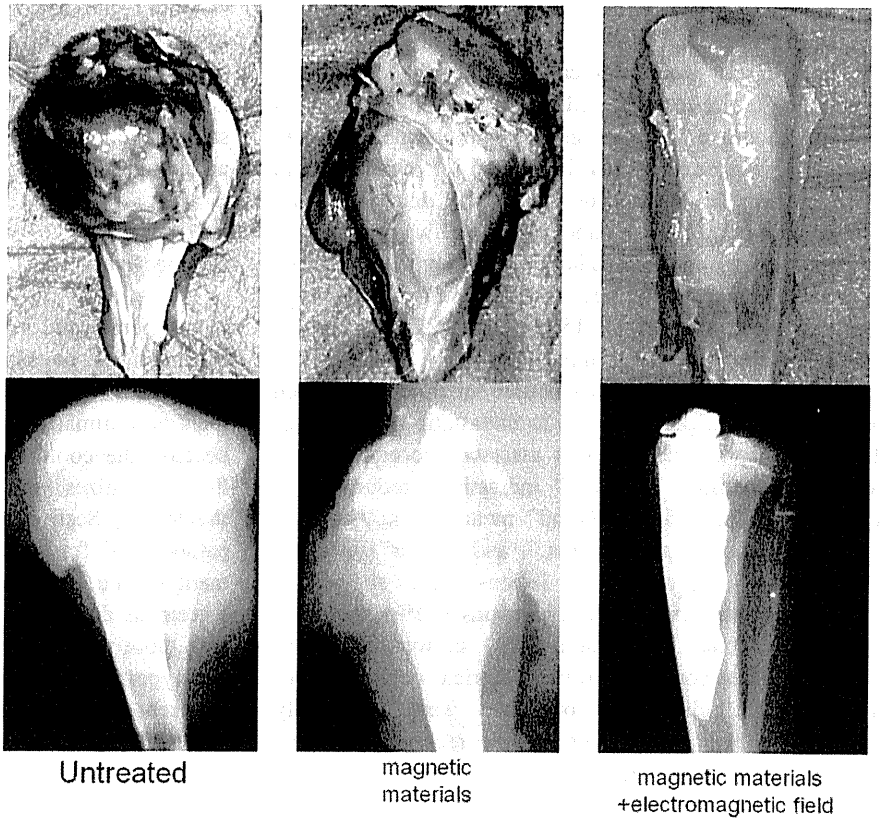

Fig. 3 The effects of hyperthermia with magnetic materials under an electromagnetic field. VX2 sarcoma cells were implanted into the tibias of rabbits. In radiographs, massive bone destruction was observed in rabbits treated with neither magnetic materials or the electromagnetic field. However, when the magnetic materials were implanted and the electromagnetic field was applied, the bone destruction was strikingly inhibited. This suggests that our new hyperthermic therapy has a prominent anti-tumor effect on metastatic bone tumors

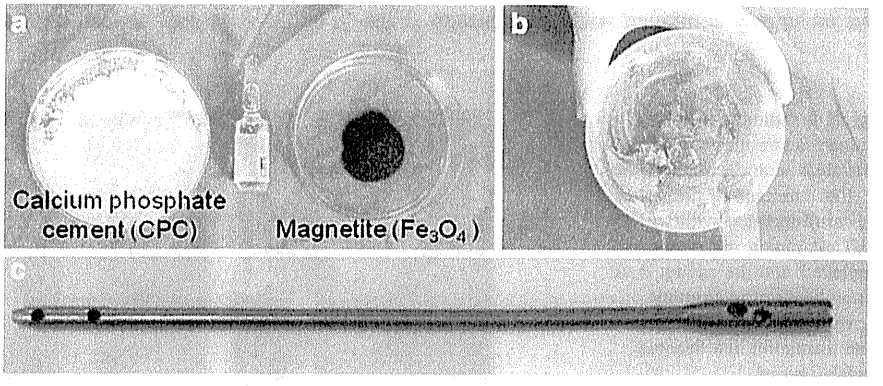

Fig. 4 The magnetic materials used for clinical appreciation of the novel therapeutic hyperthermia. **a**, **b** When the lesion was located at the metaphysis, curettage of the lesion was performed, followed by implantation of calcium phosphate cement containing magnetite into the cavity. **c** In contrast, when the lesion was located at the diaphysis, only reinforcement with an intramedullary nail was performed

containing powdered Fe_3O_4 (Fig. 4a, b) or an intramedullary nail made of a titanium alloy (Fig. 4c) as the magnetic material [21]. Because intramedullary nails made of titanium alloys have been frequently used to fix fractures all over the world, we had no legal constraints against using these nails for the patients with pathological fractures or impending fractures in Japan [33]. Calcium phosphate cement (CPC) is an injectable biocompatible bone substitute, and has been used to fill the bone defect following resection of bone tumors [34]. We have continually performed experimental studies, and found that our novel hyperthermia strategy promised good local control for bone metastasis without any adverse effects which could be detected by hematological examination and histological examination of the liver, kidneys, lungs and brain [35].

Clinical application of novel hyperthermia for bone metastases

We started clinical applications of this treatment modality from March 2003 after obtaining approval from our Institutional Ethics Investigational Review Board [21]. Our treatment strategy requires two types of treatment modalities:

an electromagnetic field generator (Fig. 1), and the magnetic materials (Fig. 4).

The surgical procedures can be categorized into two types. For the lesions located at the metaphysis, we first perform curettage of the lesion. Calcium phosphate cement containing magnetite is then implanted into the cavity. In contrast, for the lesions located at the diaphysis, only reinforcement with an intramedullary nail was performed. In both cases, hyperthermia was performed after the operation. Hyperthermic treatment was performed postoperatively on days 8, 10, 12, 15, 17, 19, 22, 24, 26 and 29. The exposure time was 15 min per day.

To date, this novel hyperthermic treatment has been performed for 23 patients with 25 metastatic bone lesions. The radiographic outcome was assessed according to the following criteria: "Excellent" indicating "reduced with visible bone formation," "Good" meaning "not progressive for more than 3 months," and "Poor" meaning "progressive". As a result, 8 lesions (32%) showed an "Excellent" outcome, while 16 lesions (64%) showed a "Good" outcome. One lesion (4%) showed a "Poor" outcome. When compared to the historical controls at our institute, the radiographic outcomes were statistically superior to those of the patients who received palliative surgery without either radiotherapy or hyperthermia, and similar to outcomes of the patients who received surgery in combination with postoperative radiotherapy. These results suggest that our novel hyperthermic therapy was as effective as surgery combined with radiotherapy (Figs. 5, 6).

With regard to complications, a sensation of heat during hyperthermia was noted by 3 patients, and tumor recurrence was observed in one patient. To our knowledge, this is the first clinical application of hyperthermia for metastatic bone tumors generated using magnetic materials and an alternating electromagnetic field.

Perspectives

Our hyperthermic strategy has several advantages for the treatment of metastatic tumors of long tubular bones compared to radiotherapy. First, our hyperthermic treatment is minimally invasive to the surrounding soft tissue, because the cooling effect of the intramuscular vascular flow minimizes soft tissue damage to the neurovascular sheath [20]. Second, our hyperthermic strategy can prevent pathological fractures because of the surgical reinforcement of the bone lesion. Moreover, this surgical reinforcement does not require any special techniques other than those routinely used by orthopedic surgeons. Finally, our hyperthermic treatment can be repeatedly applied for recurrent metastatic lesions, in contrast to radiotherapy, which cannot exceed the normal dose limitations.

This hyperthermic strategy may be applicable to other fields. Hyperthermia is already applied for the treatment of soft tissue sarcoma. The combination therapy using both cytotoxic drugs and regional hyperthermia in the treatment of soft tissue sarcoma is based upon experimental and

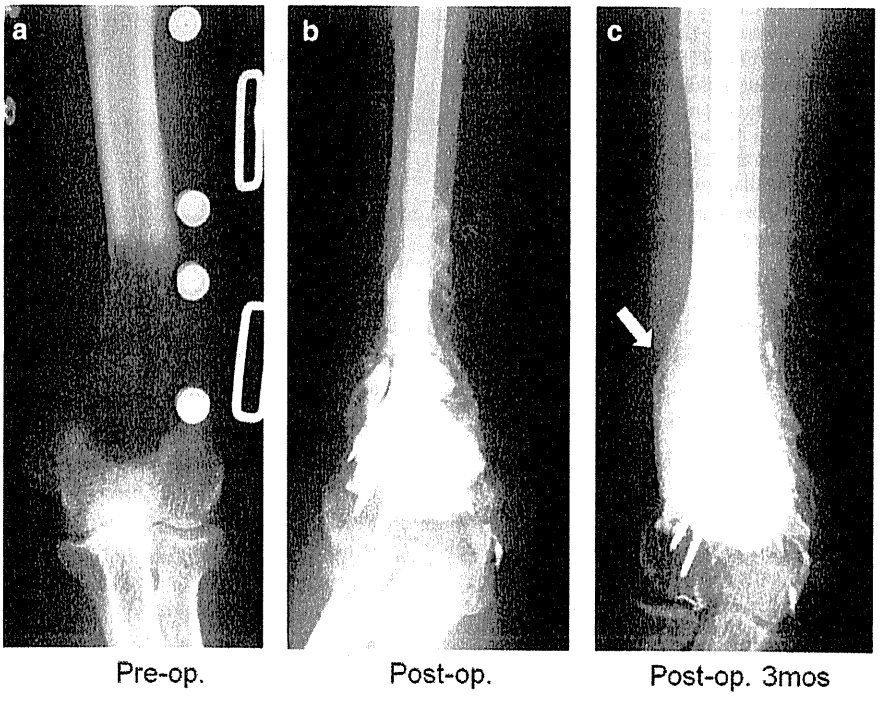

Fig. 5 A radiograph of a bladder cancer that had metastasized to the humerus (**a**). **b** After curettage of the lesion and reinforcement with wire, CPC containing magnetite was implanted into the cavity. **c** At 3 months after undergoing hyperthermia, massive new bone formation had become visible (*arrow*)

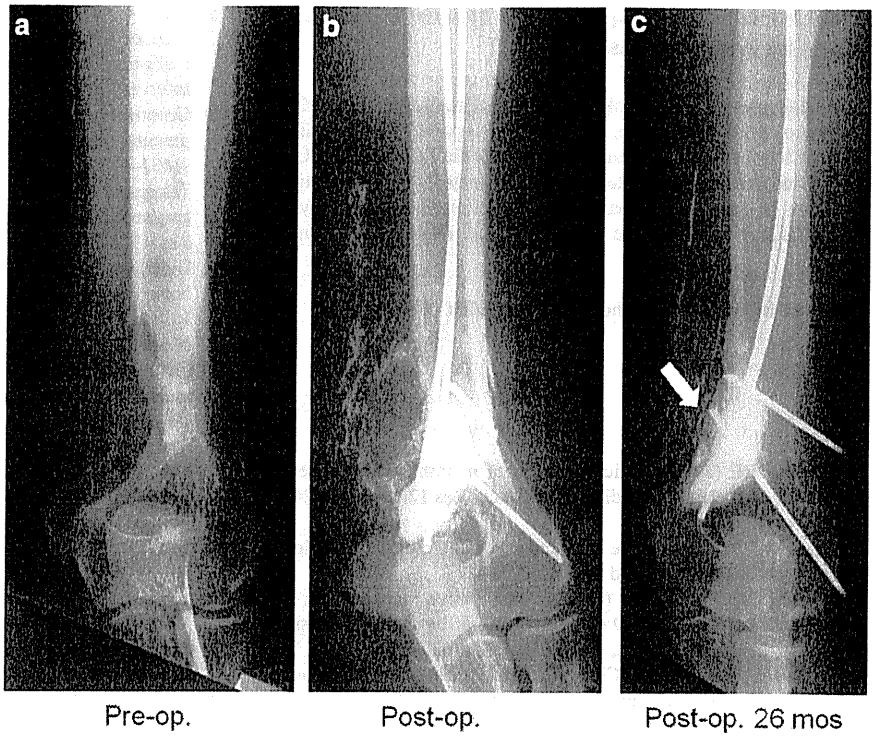

Fig. 6 A radiograph of a hepatocellular carcinoma that had metastasized to the humerus. After curettage of the lesion followed by reinforcement with wire, CPC containing magnetite was implanted into the cavity. At 26 months after undergoing hyperthermia, no recurrence was visible (*arrow*)

clinical evidence showing that heat induces tumor cell death by direct thermal toxicity and enhances the efficacy of some drugs, such as alkylating agents and platinum analogs [36, 37]. Recently micro- or nano-particles have attracted attention as a new heat source. Another new method for inducing interstitial hyperthermia is to inject a fluid containing magnetic nanoparticles intratumorally, and to apply alternating magnetic fields [23]. Kobayashi et al. [23] reported the use of magnetic cationic liposomes, where a group of cationic magnetic particles can be used as carriers to introduce magnetic nanoparticles into target cells, since their positively charged surface interacts with the negatively charged cell surface. Hyperthermia using cationic magnetic particles combined with chemotherapy or radiotherapy might also improve the therapeutic outcome of soft tissue sarcoma patients.

Despite the potential of therapeutic hyperthermia for bone metastases, there are some problems that still need to be solved. First, one of the most common sites of the metastatic bone tumors is the axial bones, including the pelvis and the spine. However, the size of the cylindrical coil of the current generator is too small to apply this hyperthermic therapy to these sites. To address this problem, we tried to make a magnetic field generator with a large coil. However, in our experiments, the increased size of the coil diminished the power of the magnetic field, and decreased the efficacy of heat induction. The design of a new and modified magnetic field generator is warranted. Second, thermal monitoring has recently evolved from the recording of the temperature at 1–8 fixed locations to real-time control based on high-density thermal profile mapping and/or non-invasive real-time characterization of temperature and distribution of physiological changes [38]. To assure its clinical effectiveness and to certify the safety of our hyperthermic treatment, effective real-time and non-invasive monitoring of the temperature is needed.

Conclusion

About two decades ago, the median survival of patients with bone metastasis from advanced lung cancer was typically measured in months, while the median survival of the patients with bone metastases from prostate cancer or breast cancer was measurable in years [39, 40]. However, recent development of new chemotherapies, including targeted therapies, has dramatically improved these patients' prognoses. Paradoxically, the improvement of prognosis of these cancer patients will lead to an increase in the number of patients with pathological fracture or impending fractures due to bone metastases, even if systemic therapy for bone metastases makes great progress. The results of our first series of clinical hyperthermia using magnetic materials achieved good local control of metastatic bone lesions. However, further investigations are

needed before this technique can be employed as a standard therapy for bone metastases.

Acknowledgments We thank the secretarial staff (Chie Usui, Chiyuki Ueno, Misa Hashimoto, Chinami Yamaguchi, Takahiro Iino, Katsura Chiba) of the Department of Orthopedic Surgery, Mie University Graduate School of Medicine, for their generous cooperation. This work is supported in part by the grant from the Ministry of Health, Labour and Welfare (Grants-in Aid for Clinical Cancer Research).

Conflict of interest No author has any conflict of interest.

References

1. Coleman RE (2006) Clinical features of metastatic bone disease and risk of skeletal morbidity. Clin Cancer Res 12(Suppl):S6243–S6249
2. Fidler M (1981) Incidence of fracture through metastases in long bones. Acta Orthop Scand Dec 52:623–627
3. Frassica DA, Frassica FJ (1998) Nonoperative management. In: Simon MA, Springfield D (eds) Surgery for bone and soft-tissue tumors. Lippincott-Raven, Philadelphia, pp 633–637
4. Yazawa Y, Frassica FJ, Chao EY et al (1990) Metastatic bone disease. A study of the surgical treatment of 166 pathologic humeral and femoral fractures. Clin Orthop Relat Res 251:213–219
5. van der Zee J (2002) Heating the patient: a promising approach? Ann Oncol 13:1173–1184
6. Harmon BV, Corder AM, Collins RJ et al (1990) Cell death induced in a murine mastocytoma by 42–47 degrees C heating in vitro: evidence that the form of death changes from apoptosis to necrosis above a critical heat load. Int J Radiat Biol 58:845–858
7. Robins HI, D'Oleire F, Grosen E et al (1997) Rationale and clinical status of 41.8 degrees C systemic hyperthermia tumor necrosis factor, and melphalan for neoplastic disease. Anticancer Res 17:2891–2894
8. Sellins KS, Cohen JJ (1991) Hyperthermia induces apoptosis in thymocytes. Radiat Res 126:88–95
9. Rau B, Wust P, Hohenberger P et al (1998) Preoperative hyperthermia combined with radiochemotherapy in locally advanced rectal cancer: a phase II clinical trial. Ann Surg 227:380–389
10. Grunhagen DJ, de Wilt JH, Graveland WJ et al (2006) Outcome and prognostic factor analysis of 217 consecutive isolated limb perfusions with tumor necrosis factor-alpha and melphalan for limb-threatening soft tissue sarcoma. Cancer 106:1776–1784
11. Fan QY, Ma BA, Qlu XC et al (1996) Preliminary report on treatment of bone tumors with microwave-induced hyperthermia. Bioelectromagnetics 17:218–222
12. Sakurai H, Hayakawa K, Mitsuhashi N et al (2002) Effect of hyperthermia combined with external radiation therapy in primary non-small cell lung cancer with direct bony invasion. Int J Hyperthermia 18:472–483
13. Malawer MM, Marks MR, McChesney D et al (1988) The effect of cryosurgery and polymethylmethacrylate in dogs with experimental bone defects comparable to tumor defects. Clin Orthop Relat Res 226:299–310
14. Sturup J, Nimb L, Kramhoft M et al (1994) Effects of polymerization heat and monomers from acrylic cement on canine bone. Acta Orthop Scand 65:20–23
15. Kusaka M, Takegami K, Sudo A et al (2002) Effect of hyperthermia by magnetite cement on tumor-induced bone destruction. J Orthop Sci 7:354–357
16. Vogl TJ, Mack MG, Straub R et al (2001) MR-guided laser-induced thermotherapy of the infratemporal fossa and orbit in malignant chondrosarcoma via a modified technique. Cardiovasc Intervent Radiol 24:432–435
17. Groenemeyer DH, Schirp S, Gevargez A (2002) Image-guided percutaneous thermal ablation of bone tumors. Acad Radiol 9:467–477
18. Takegami K, Sano T, Wakabayashi H et al (1998) New ferromagnetic bone cement for local hyperthermia. J Biomed Mater Res 43:210–214
19. Uchida A, Wakabayashi H, Okuyama N et al (2004) Metastatic bone disease: pathogenesis and new strategies for treatment. J Orthop Sci 9:415–420
20. Morita K, Morita S, Tsujiguchi M et al (2002) A method of local hyperthermia with ferromagnetic bone cement. Improvement for clinical medicine. Orthopaedic Ceramic Implants 19–20:97–100
21. Matsumine A, Kusuzaki K, Matsubara T et al (2007) Novel hyperthermia for metastatic bone tumors with magnetic materials by generating an alternating electromagnetic field. Clin Exp Metastasis 24:191–200
22. Ivkov R, DeNardo SJ, Daum W et al (2005) Application of high amplitude alternating magnetic fields for heat induction of nanoparticles localized in cancer. Clin Cancer Res 11:7093s–7103s
23. Ito A, Shinkai M, Honda H et al (2005) Medical application of functionalized magnetic nanoparticles. J Biosci Bioeng 100:1–11
24. Kawashita M, Tanaka M, Kokubo T et al (2005) Preparation of ferrimagnetic magnetite microspheres for in situ hyperthermic treatment of cancer. Biomaterials 26:2231–2238
25. Yan S, Zhang D, Gu N et al (2005) Therapeutic effect of Fe_2O_3 nanoparticles combined with magnetic fluid hyperthermia on cultured liver cancer cells and xenograft liver cancers. J Nanosci Nanotechnol. 5:1185–1192
26. Hilger I, Hergt R, Kaiser WA (2000) Effects of magnetic thermoablation in muscle tissue using iron oxide particles: an in vitro study. Invest Radiol 35:170–179
27. Johannsen M, Gneveckow U, Eckelt L et al (2005) Clinical hyperthermia of prostate cancer using magnetic nanoparticles: presentation of a new interstitial technique. Int J Hyperthermia 21:637–647
28. Kokubo T (1991) Bioactive glass ceramics: properties and applications. Biomaterials 12:155–163
29. Kapp DS (1989) Indications for the clinical use of deep local and regional hyperthermia in conjunction with radiation therapy. Strahlenther Onkol 165:724–728
30. Ikenaga M, Ohura K, Kotoura Y et al (1994) Hyperthermic treatment of canine tibia through RF inductive heating of an intramedullary nail: a new experimental approach to hyperthermia for metastatic bone tumours. Int J Hyperthermia 10:507–516
31. Ikenaga M, Ohura K, Yamamuro T et al (1993) Localized hyperthermic treatment of experimental bone tumors with ferromagnetic ceramics. J Orthop Res 1:849–855
32. Kawanabe K, Tamura J, Yamamuro T et al (1993) A new bioactive bone cement consisting of BIS-GMA resin and bioactive glass powder. J Appl Biomater 4:135–141
33. Akagi M, Tsuboyama T, Ikenaga M et al (1997) Anti-tumour effects of localized hyperthermia on an experimental bone tumour using an intramedullary nail. Int J Hyperthermia 13:387–400
34. Matsumine A, Kusuzaki K, Matsubara T et al (2006) Calcium phosphate cement in musculoskeletal tumor surgery. J Surg Oncol 93:212–220
35. Morita K, Uchida A (2002) The treatment of bone tumors with the local hyperthermia using calcium phosphate cement containing ferromagnetite. J Musculoskelet Syst 15:443–445

36. Pennacchioli E, Fiore M, Gronchi A (2009) Hyperthermia as an adjunctive treatment for soft-tissue sarcoma. Expert Rev Anticancer Ther 9:199–210
37. Otsuka T, Yonezawa M, Kamiyama F et al (2001) Results of surgery and radio-hyperthermo-chemotherapy for patients with soft-tissue sarcoma. Int J Clin Oncol. 6:253–258
38. Stauffer PR (2005) Evolving technology for thermal therapy of cancer. Int J Hyperthermia 21:731–744
39. Coleman R, Rubens R (1987) The clinical course of bone metastases in breast cancer. Br J Cancer 77:336–340
40. Fan K, Peng CF (1983) Predicting the probability of bone metastasis through histological grading of prostate carcinoma: a retrospective correlative analysis of 81 autopsy cases with antemortem transurethral resection specimen. J Urol 130:708–711

FOOT & ANKLE INTERNATIONAL

DOI: 10.3113/FAI.2011.0905

Recurrent Ankle Equinus Deformity Due to Intramuscular Hemangioma of the Gastrocnemius: Case Report

Tomoki Nakamura, MD[1]; Akihiko Matsumine, MD[1]; Masaki Nishiyama, MD[2]; Atsumasa Uchida, MD[1]; Akihiro Sudo, MD[1]
Mie, Japan

Level of Evidence: V, Expert Opinion

Key Words: Intramuscular Hemangioma; Gastrocnemius; Ankle Equinus

INTRODUCTION

Acquired ankle equinus is not so uncommon. A neurological deficit causing muscle wasting and contracture should be ruled out. For example, spasm or contracture of the gastrocnemius muscle is predominantly responsible for the equinus deformity of the foot in cerebral palsy.[3,4] In addition, there are other causes of equinus deformity, such as poliomyelitis, trauma, diabetes, muscular dystrophy, diastrophic dysplasia, or idiopathic.[2–5,9,10] Many surgical procedures have been described for the treatment of this deformity including gastrocnemius recession or tendoachilles lengthening if it is not corrected by conservative treatment.[2,3] This report presents the case of a patient who complained of popliteal pain and a fourth recurrence of ankle equinus with the presumed diagnosis of idiopathic shortening of the tendoachilles over the course of 23 years which was actually due to intramuscular hemangioma of the gastrocnemius.

[1]Department Of Orthopaedic Surgery, Mie Graduate School Of Medicine, Mie, Japan.
[2]Department Of Orthopaedic Surgery, Mie Hospital, Mie, Japan.

One or more of the authors has received or will receive benefits for personal or professional use from a commercial party related directly or indirectly to the subject of this article.

Corresponding Author:
Akihiko Matsumine, MD
Department of Orthopaedic Surgery
Mie University Graduate School of Medicine
Mie 514-8507 Edobashi
2-174 Tsu-city
Mie
Japan
E-mail: matsumin@clin.medic.mie-u.ac.jp

CASE REPORT

A 35-year-old female presented to our clinic because of recurrent left ankle equinus deformity with severe popliteal pain with walking. She had previously undergone four previous open tendoachilles lengthening procedures for left ankle equinus deformity with the diagnosis of idiopathic shortening of the tendoachilles. The first operation was performed when she was 12 years old, the second at 15, and the third at 18, and the fourth at 33 years of age. However, severe pain with walking persisted and ankle equinus recurred within 6 months after each surgery. Physical examination revealed a rigid 30-degree left ankle equinus deformity when the knee was extended (Figure 1A). But, the ankle could be dorsiflexed to neutral when the knee was flexed (Figure 1B). Although no distinct mass was clinically evident in the left popliteal or proximal leg region, point tenderness was found at the lateral side of the proximal calf. She used two crutches to walk due to severe pain. The right ankle could be dorsiflexed to 20 degrees with the knee in full extension. Radiographs of the leg showed no ectopic calcifications. An MRI showed a soft-tissue mass measuring 5 cm × 2 cm within the lateral gastrocnemius muscle with intermediate signal-intensity on T1-weighted images and heterogeneous high signal-intensity on T2-weighted images, suggesting a cavernous hemangioma (Figure 2). Because the tumor seemed to be the responsible for the recurrent ankle equinus deformity of this patient, it was widely resected, including the whole lateral gastrocnemius (Figure 3) and a lateral small part (about 10%) of the medial gastrocnemius via an S-shaped posterior approach. Additionally, the residual medial gastrocnemius aponeurosis was released. The histological subtype of intramuscular hemangioma was cavernous hemangioma (Figure 4). After completion of surgery, the ankle was immobilized at 20 degrees of ankle dorsiflexion and 10 degrees of knee flexion using long leg cast for 1 week. The long leg cast was removed on postoperative day 7 when she was allowed full weightbearing. After 2 years followup, the patient has regained normal range of ankle dorsiflexion with full knee extension (Figure 5), and a normal heel-toe gait without any pain. There has been no recurrence of tumor on MRI.

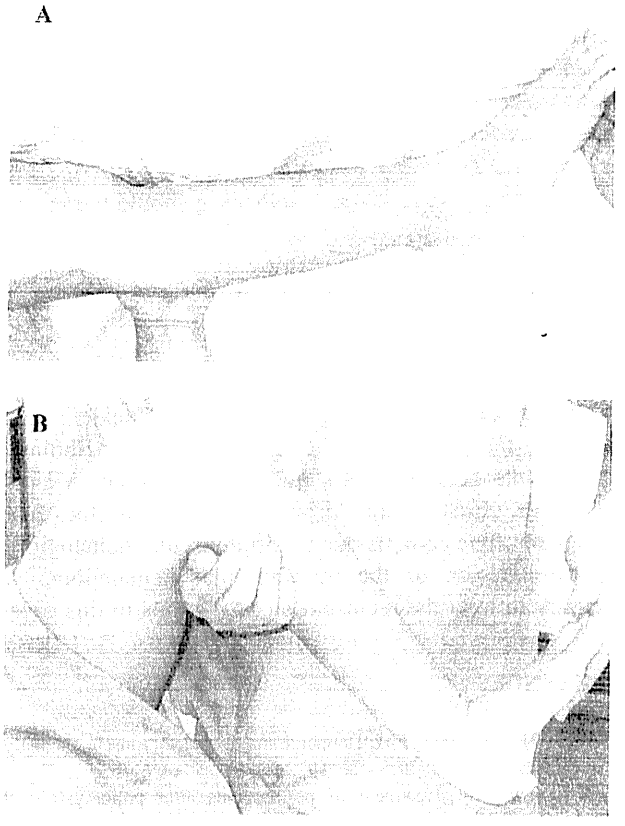

Fig. 1: A, A rigid 30-degree left ankle contracture with the knee extended. B, The ankle dorsiflexed to neutral with the knee flexed.

DISCUSSION

Although acquired unilateral ankle equinus deformity is not so uncommon, we experienced an unusual case with a multiply recurrent ankle equinus deformity caused by intramuscular hemangioma in the calf muscle.[6,12,15] The diagnosis of hemangioma is indeed difficult when it is not palpable. In the current case, her previous doctors did not consider that the shortening of the gastrocsoleus was due to intramuscular hemangioma because no mass was palpable.

Fig. 3: Gross appearance of the resected tumor including normal gastrocnemius muscle tissue.

Contracture of the gastrocnemius can be confirmed by performing the Silfverskiold test:[11] if the equinus is due mainly to gastrocnemius contracture, it can be readily overcome by flexing the knee which relaxes the gastrocnemius (including the current case). If this is not the case, the deformity may also be due to contracture of the soleus, long toe flexors, tibialis posterior or peroneal muscles, or contracture of the posterior capsule of the ankle joint or occasionally bony deformity.

We strongly suspected that shortening of the tendoachilles was due to the lesion located in lateral head of gastrocnemius because the Silfverskiold test was positive.

Intramuscular hemangiomas account for only 0.8% of hemangiomas.[13,14] The most common location is the lower extremities, followed by the upper extremities and head and neck. They tend to appear in adolescence or young

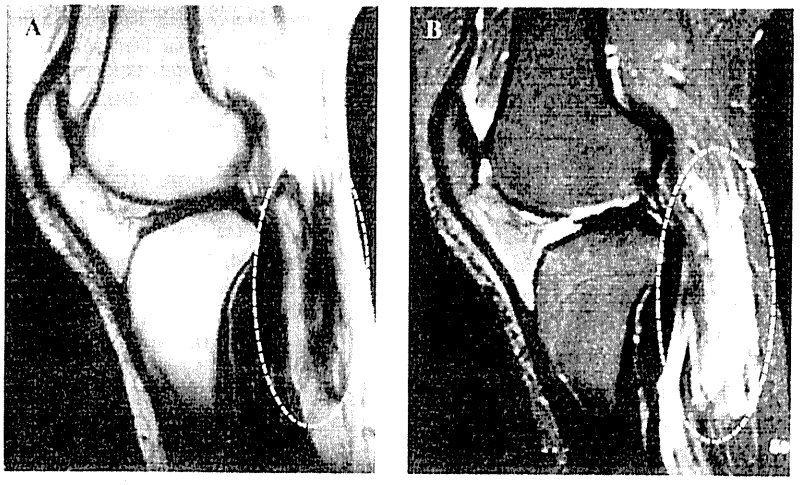

Fig. 2: MRI showed an intramuscular tumor within the lateral gastrocnemius muscle with intermediate signal-intensity on T1-weighted images (A) and heterogeneous high signal-intensity on T2-weighted images (B).

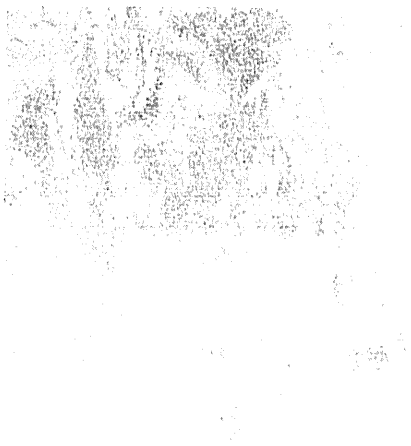

Fig. 4: Histopathologic findings revealed a cavernous intramuscular hemangioma (hematoxylin and eosin stain; magnification, ×4).

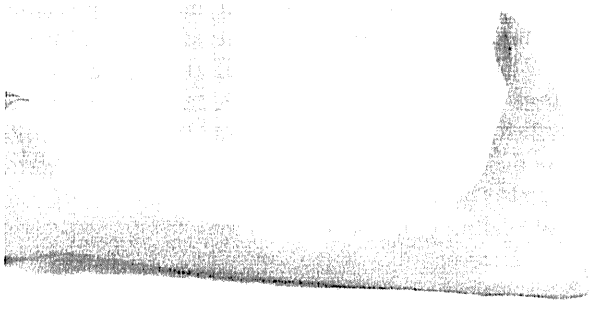

Fig. 5: The patient has regained a normal range of ankle movement with the knee extended.

adulthood.[8] The natural history of many hemangiomas is they remain relatively dormant until they are stimulated by a trigger event, such as trauma or pregnancy. Pain is main symptom occurring in 60% of cases. Tumor mass is present in most patients (found in 98%).[1] In the current case, there was no history of trauma or pregnancy during her previous four surgeries. Deeply situated hemangiomas that arise in the deep subcutaneous layer and muscle pose diagnostic difficulties. In the current case, a distinct, tender point was observed at the lateral side of the proximal calf. We found a careful examination was necessary for the diagnosis of this intramuscular hemangioma.

MRI has been proposed as the optimal diagnostic test when an intramuscular hemangioma is strongly suspected.[13–15] The MRI findings in the current case allowed the preoperative diagnosis. When intramuscular hemangioma is symptomatic, surgical excision can become the treatment option. Allen and Enzinger reported that 18% of the patients had a local recurrence and 7% had more than one recurrence.[1] Therefore, en-bloc excision with surrounding muscle is recommended to prevent local recurrence.

Klemme et al. reported that open tendoachilles lengthening can provide acceptable results with minimal immobilization for ankle equinus caused by hemangioma.[6] However, ankle equinus recurred after the fourth open tendoachilles lengthening procedure in the current patient. Therefore, surgical excision was necessary to prevent recurrence of the ankle equinus. Open tendoachilles lengthening should therefore be considered if tumor resection alone fails to regain adequate ankle motion.

CONCLUSION

If there are no neurological causes of ankle equinus deformity, the possibility of soft tissue tumor including an intramuscular hemangioma should be considered. A careful physical examination should provide important clues to the etiology of ankle equinus due to intramuscular hemangioma.. Surgical excision of the intramuscular hemangioma was necessary to treat the recurrent ankle equinus in this case.

REFERENCES

1. **Allen, PB; Enzinger, FM:** Hemangioma of skeletal muscle: an analysis of 89 cases. Cancer. **29:**8–22, 1972.
2. **Arslanova, AV:** Treatment of pes equinus after poliomyelitis. Sov Zdravookhr Kirg. **4:**25–28, 1965.
3. **Borton, DC; Walker, K; Pirpiris, M; et al.:** Isolated calf lengthening in cerebral palsy. J Bone Joint Surg. **83-B:**364–370, 2001.
4. **Craig, JJ; Vuren, VV:** The importance of gastrocnemius recession in the correction of equinus deformity in cerebral palsy. J Bone Joint Surg Br. **58-B:**84–87, 1976.
5. **Kent, MH:** Ankle equinus related to trauma, and its surgical treatment: a preliminary report of three cases. J Foot Surg. **17:**75–79, 1978.
6. **Klemme, WR; James, P; Skinner, SR:** Latent onset unilateral toe-walking secondary to hemangioma of the gastrocunemius. J Pediatr Orthop. **14:**773–775, 1994.
7. **Lavery, LA; Armstrong, DG; Boulton, AJ:** Ankle equinus deformity and its relashionship to high plantar pressure in a large population with diabetes mellitus. J Am Podiatr Med Assoc. **92:**479–482, 2002.
8. **Ranero-Juarez, AG; Rosales-Galindo, VM; Leon-Takahashi, AM; et al.:** Intramuscular hemangiomas of the extremities: report of six cases. Int J Dermatol. **48:**875–878, 2009.
9. **Read, L; Galasko, CSB:** Delay in diagnosing Duchenne muscular dystrophy in orthopaedic clinics. J Bone Joint Surg. **68-B:**481–482, 1986.
10. **Ryoppy, S; Poussa, M; Merikanto, J; et al.:** Foor deformities in diastrophic dysplasia. An analysis of 102 patients. J Bone Joint Surg. **74-B:**441–444, 1992.
11. **Silfverskiold, N:** Reduction of the uncrossed two-joints muscles of the leg to one-joint muscles in spastic conditions. Acta Cbir Scand. **56:**315–328, 1924.
12. **Sutherland, AD:** Equinus deformity due to haemangioma of calf muscle. J Bone Joint Surg. **57-B:**104–105, 1975.
13. **Watson, WL; McCarthy, WD:** Blood and lymph vessel tumor. A report of 1056 cases. Surg Gynecol Obstet. **71:**569–588, 1940.
14. **Welsch, D; Hengerer, AS:** The diagnosis and treatment of intramuscular hemangiomas of the masseter muscle. Am J Otolaryngol. **1:** 186, 1980.
15. **Wu, JL; Wu, CC; Wang, SJ; et al.:** Imaging strategies in intramuscular haemangiomas: an analysis of 20 cases. Int Orthop. **31:** 569–575, 2007.

Biochemical and Biophysical Research Communications 407 (2011) 525–530

Contents lists available at ScienceDirect

Biochemical and Biophysical Research Communications

journal homepage: www.elsevier.com/locate/ybbrc

TNF inhibitor suppresses bone metastasis in a breast cancer cell line

Takahiko Hamaguchi [1], Hiroki Wakabayashi *,[1], Akihiko Matsumine, Akihiro Sudo, Atsumasa Uchida

Department of Orthopaedic Surgery, Mie University Graduate School of Medicine, Japan

ARTICLE INFO

Article history:
Received 10 March 2011
Available online 15 March 2011

Keywords:
Infliximab
Tumor necrosis factor-alpha
Breast cancer
MDA-MB-231
Bone metastasis

ABSTRACT

In the evolution of cancer, tumor necrosis factor-alpha (TNF-α) plays a paradoxical role. High doses induce significant anticancer effects, but conversely, physiologic and pathologic levels of TNF-α may be involved in cancer promotion, tumor growth, and metastasis.

Infliximab is a chimeric murine monoclonal antibody that binds with high affinity to soluble and membrane TNF-α and inhibits binding of TNF-α to its receptors. In the present study, we investigated the effect of infliximab, a TNF-α antagonist, on breast cancer aggressiveness and bone metastases.

Infliximab greatly reduced cell motility and bone metastases in a metastatic breast cancer cell line, MDA-MB-231. The mechanism of bone metastasis inhibition involved decreased expression of CXC chemokine receptor 4 (CXCR4) and increased expression of decorin, which is the prototype of an expanding family of small leucine-rich proteoglycans. These results suggest a novel role for TNF-α inhibition in the reduction or prevention of bone metastases in this breast cancer model. Our study suggests that inhibition of TNF-α using infliximab may become a preventive therapeutic option for breast cancer.

1. Introduction

Breast cancer metastasizes to bone in more than 80% of patients with advanced disease [1]. A recent study showed that the presence of isolated tumor cells in bone marrow at the time of diagnosis of breast cancer is associated with a poor prognosis [2]. Tumor growth at the bone site can be extremely painful due to the presence of tumor mass in the bone-marrow cavity and to nerve compression. Metastasized tumor growth at the bone site can lead to debilitating fractures of, particularly, the hip and spine [3].

Tumor necrosis factor-alpha (TNF-α) plays a paradoxical role in the evolution of cancer. It can act as a tumor necrosis factor and also as a tumor-promoting factor [4]. Local administration of high-dose TNF-α is antiangiogenic and has a powerful antitumor effect [5]. On the other hand, endogenous TNF-α chronically produced in the tumor microenvironment enhances tumor development and spread.

TNF-α, a major inducer of chemokines, is a key player in the tumor microenvironment and is involved in the pathogenesis of breast cancer [6]. TNF-α also stimulates the production of interleukin-6 (IL-6), and it is a potent growth factor and directly stimulates angiogenesis [7]. It is also an important factor for breast cancer progression [8]. High serum TNF-α concentration in breast cancer patients correlates with aggressive tumor biology [9].

Infliximab is a chimeric human-mouse monoclonal antibody consisting of human immunoglobulin G1 (IgG1) Fc regions fused to the variable Fv region of a high-affinity neutralizing murine antihuman TNF antibody [10]. It prevents the binding of TNF-α to its receptors, TNF-R1 (p55 receptor) and TNF-R2 (p75 receptor), and causes cell death via complement-mediated lysis through interaction with membrane-bound TNF-α [11]. Infliximab is well tolerated, is licensed for use in Crohn's disease and rheumatoid arthritis at doses of 3–10 mg/kg, and has been used in more than 750,000 patients worldwide.

Neutralization of TNF-α results in reduction of TNF-α-regulated cytokines, proteases, and other growth factors at the inflammatory site, minimizing clinical symptoms and thus reversing the clinical disease [12,13].

In the present study, the effect of infliximab on bone metastases of a breast cancer cell line (MDA-MB-231) was investigated in vitro and in vivo.

2. Materials and methods

2.1. Reagents

Infliximab was purchased from Mitsubishi Tanabe K.K. (Tokyo, Japan). Rabbit polyclonal antibodies to phospho-NF-κB, phospho-SPAK/JNK and CXC chemokine receptor 4 (CXCR4) were from Cell Signaling Technology (Danvers, MA). Goat polyclonal antibody to decorin was from R&D Systems (Minneapolis, MN). Goat polyclonal

* Corresponding author. Address: Department of Orthopaedic Surgery, Mie University Graduate School of Medicine, 2-174, Edobashi, Tsu, Mie 514-8507, Japan. Fax: +81 059 231 5211.
E-mail address: whiroki@clin.medic.mie-u.ac.jp (H. Wakabayashi).

[1] These authors contributed equally to this work.

0006-291X/$ - see front matter © 2011 Elsevier Inc. All rights reserved.
doi:10.1016/j.bbrc.2011.03.051

antibody to actin was from Santa Cruz Biotechnology (Santa Cruz, CA).

2.2. Cell culture

The human breast cancer cell lines MDA-MB-231 (MDA-231), MCF7, and ZR-75-1 were obtained from the American Type Culture Collection (ACTT, Manassas, VA). MDA-231 cells were cultured in Dulbecco's modified Eagle's medium (DMEM) supplemented with 10% fetal bovine serum (FBS), and grown in a 5% CO_2 atmosphere at 37 °C. MCF7 and ZR-75-1 were cultured in RPMI medium 1640 supplemented with 10% FBS.

2.3. Animals

Five-week-old female BALB/c nu/nu mice (SLC, Hamamatsu, Japan) were used for all in vivo experiments. Procedures involving animals and their care were conducted in conformity with national and international laws and policies and approved by our Institutional Review Board.

2.4. Reverse transcriptase-polymerase chain reaction

For investigation of the expression of mRNA, total RNA was isolated using ISOGEN and treated with DNase (Wako Pure Chemical Industries, Japan). cDNA was synthesized using PrimeScript Reverse Transcriptase (Takara Bio, Shiga, Japan). PCR amplification was performed using the following specific primers and cycling parameters: human TNF-α, forward primer 5-GTGGCAGTCTCAAACTGA-3, reverse primer, 5-TATGGAAAGGGGCACTGA-3, 30 s at 94 °C, 30 s at 58 °C, 30 s at 72 °C for 35 cycle; human TNF-R1, forward primer 5-TCGATTTGCTGTACCAAGT-3, reverse primer 5-GAAAATGACCAGGGGCAACAG-3, 30 s at 94 °C, 30 s at 56 °C, 30 s at 72 °C for 35 cycles; human TNF-R2, forward primer 5-CAGTGCGTTGGACAGAAG-3, reverse primer 5-GGCTTCATCCCAGCATCA-3, 30 s at 94 °C, 30 s at 60 °C, 30 s at 72 °C for 35 cycles; and human glyceraldehyde-3-phosphate dehydrogenase (GAPDH), forward primer 5-CATGGAGAAGGCTGGGGCTC-3, reverse primer 5-CACTGACACGTTGGCAGTGG-3, 30 s at 94 °C, 30 s at 55 °C, 30 s at 72 °C for 35 cycles. The PCR products were loaded in 2% agarose gel and stained with ethidium bromide. The size of the fragments was confirmed by reference to a 100-bp DNA ladder.

2.5. ELISA

ELISA tests were used to determine the TNF-α levels in MDA-231, MCF7, and ZR-75-1. Each of the 3 cell lines (1×10^4) was plated in 48-well plates. At near confluence, the cells were rinsed with PBS, and 250 μl of serum-free DMEM were added to each well. The conditioned medium was collected after 48 h. Concentrations of TNF-α in the conditioned medium were determined by ELISA using the Quantikine TNF-α kit (R&D Systems) according to the manufacturer's instructions.

2.6. SDS–PAGE and immunoblotting

Western blots were performed as described previously [14]. Briefly, samples (cell lysates) were separated by SDS–PAGE, transferred to nitrocellulose membranes, and immunoblotted with primary antibodies. The primary antibodies were polyclonal rabbit antiserum against phospho-NF-κB, polyclonal rabbit antiserum against phospho-SAPK/JNK, polyclonal rabbit antiserum against CXCR4, polyclonal goat antiserum against decorin, and polyclonal goat antiserum against β-actin.

Separated proteins were visualized with horseradish peroxidase-conjugated anti-rabbit antibody or anti-goat antibody (Dako Cytomation, Carpinteria, CA) with enhancement by chemiluminescence using ECL+ (Amersham Pharmacia Biotech, Arlington Heights, IL); chemiluminescence detection used LAS-1000 plus (Fujifilm, Tokyo, Japan), in accordance with the manufacturer's specifications.

2.7. Cell proliferation assay

The cell lines were seeded in duplicate at a density of 3.0×10^4 cells/well in 6-cm plates. Cells were trypsinized and counted with a Coulter Counter (Beckman Coulter, Fullerton, CA) at 24, 48, 72, and 96 h after seeding.

2.8. Migration and invasion assay

Cell migration and invasion analyses using Boyden chambers were performed as described previously [14]. The two compartments were separated by a polyethylene terephthalate membrane (6-mm diameter, 8-μm pore size; Falcon Cell Culture Inserts; Becton Dickinson Labware, Franklin Lakes, NJ, USA). Two types of assay were conducted: a simple migration assay, for which the filter was not coated with Matrigel; and a migration and invasion assay, for which the filters were coated with Matrigel matrix. Briefly, cells were added to the upper compartment of the chamber. The chambers were incubated for 24 h, then cells on the upper surface of the membrane were thoroughly removed with a cotton swab. Quantification was performed by staining membranes with a Diff-Quik kit (Sysmex, Hyogo, Japan) and determining the mean number of cells that had migrated to the lower surface of the membrane. A high-power (400×) field was used. Ten randomly chosen areas on each filter were used to obtain the mean cell number. Each assay was performed ten times.

2.9. Intracardiac experimental metastasis model

Subconfluent cells were fed with fresh medium 24 h before intracardiac injection. Cells (1×10^5) were suspended in 0.1-ml sterile PBS and injected with a 29-gauge needle into the left ventricle of 5-week-old female nude mice under anesthesia with pentobarbital (0.05 mg/g). Animals were maintained in accordance with the guidelines of the Institutional Animal Care and Use Committee.

2.10. Effect of infliximab on bone metastasis in vivo

Infliximab was administered intraperitoneally at a dose of 10 mg/kg on days 2, 9, 16, and 23 after tumor cell inoculation. Untreated mice received saline by intraperitoneal injection. Mice were sacrificed 4 weeks after inoculation. X-ray and pathology examinations of bilateral hindlimbs were conducted.

2.11. Radiographic analysis of bone metastasis

Development of bone metastasis was monitored by X-ray imaging 4 weeks after tumor inoculation as described previously [14]. All radiographs were analyzed carefully by three orthopedists. The number of bone metastases per femur and tibia was determined for each mouse, and osteolytic lesions in the femur and tibia were measured using NIH-Image 1.62b7 image analysis software. Data are shown as number of metastases per mouse or as metastasis area (mm^2) per hindlimb bone (femur and tibia).

2.12. Histological examination

Mice were sacrificed 4 weeks after intracardiac inoculation of tumor cells. Bilateral hindlimbs were removed and fixed in 4% paraformaldehyde for 1 day. Femurs and tibias were decalcified